Optical Engineering

OpticalEngineering.SPIEDigitalLibrary.org

Quantitative analysis of water content and distribution in plants using terahertz imaging

Anton V. Shchepetilnikov
Alexey M. Zarezin
Viacheslav M. Muravev
Pavel A. Gusikhin
Igor V. Kukushkin

SPIE.

Anton V. Shchepetilnikov, Alexey M. Zarezin, Viacheslav M. Muravev, Pavel A. Gusikhin, Igor V. Kukushkin, "Quantitative analysis of water content and distribution in plants using terahertz imaging," *Opt. Eng.* **59**(6), 061617 (2020), doi: 10.1117/1.OE.59.6.061617

Quantitative analysis of water content and distribution in plants using terahertz imaging

Anton V. Shchepetilnikov,[a,b,*] Alexey M. Zarezin,[a,b,c] Viacheslav M. Muravev,[a,b] Pavel A. Gusikhin,[a,b] and Igor V. Kukushkin[a,b]

[a]Russian Academy of Sciences, Institute of Solid State Physics, Chernogolovka, Russia
[b]TeraSense Group, Inc., San Jose, California, United States
[c]Moscow Institute of Physics and Technology, Dolgoprudny, Russia

Abstract. Quantitative analysis of the temporal evolution and spatial distribution of water content in grass and clover leaves has been carried out *in vivo*, with the aid of the terahertz imaging system comprised of an impact avalanche and transit time-diode source, a condenser lens, and an imaging camera. The leaf samples were exposed to 100-GHz radiation to measure the transmitted power. Progressive variation in the level of the transmitted signal has been detected when the plants were subject to the condition of insufficient water supply, whereas after watering the plants, the transmission was restored to its initial value. The presented experimental results demonstrate that TeraSense imaging instrumentation can be effectively used to monitor the hydration state of plants in their natural environment. © *2020 Society of Photo-Optical Instrumentation Engineers (SPIE)* [DOI: 10.1117/1.OE.59.6.061617]

Keywords: terahertz imaging; plants hydration status.

Paper 191486SS received Oct. 25, 2019; accepted for publication Jan. 3, 2020; published online Jan. 22, 2020.

1 Introduction

Terahertz (THz) radiation corresponds to the electromagnetic spectrum between 0.1 and 1 THz (1 to 100 meV). Many molecules exhibit strong absorption in the THz frequency band due to their rotational and vibrational transitions. This molecular property opens up promising opportunities for various prospective applications of THz imaging in bioscience.[1] Possible practical areas of interest may include noninvasive detection of cells and tissues,[2,3] nondestructive crop and seed separation,[4,5] and monitoring water content in living cells of humans and plants.[6] To make the transition from a laboratory-scale terahertz imaging technique to an industrial-grade technology, the slow and cumbersome, single-pixel, raster-scanning systems need to be replaced with fast, cutting-edge multipixel cameras. Such advanced imaging systems become particularly critical in high-throughput conveyor applications. In this paper, we present a detailed study of the evolution of plant hydration accomplished employing a semiconductor multipixel THz camera. The primary objective of our investigation has been to make terahertz technology more practical and versatile for a broad range of bioscience applications.

The level of water content in plants is one of the key parameters to monitor at nearly every stage of their cultivation process. On the one hand, inadequate hydration can lead to a significant reduction in the quality and quantity of the yield, whereas prolonged or severe water stress may even result in the death of the crop. On the other hand, over-irrigation is not only economically inefficient due to excessive use of water resources but can also harm the plants by impairing soil aeration and thereby increasing their vulnerability to certain pests and diseases. Therefore, it is vital to determine the acceptable dehydration level of a plant not to be destructive to it or to undermine its normal growth and productiveness.

Traditionally, the hydration state of a plant as a whole is monitored by measuring the water content of its leaves.[7] This quantity can be extracted from the analysis of their transmission and

*Address all correspondence to Anton V. Shchepetilnikov, E-mail: shchepetilnikov@issp.ac.ru

reflection data obtained in the terahertz (THz) frequency range. Unlike most dehydrated biological tissues that are transparent to THz radiation, water is extremely adsorbent in this frequency range.[8,9] Thus, even relatively small variations of water amount contained in the leaves result in drastic changes in their THz optical properties.[6,10–14] Such fluctuations can be sensed easily by means of contemporary THz imaging techniques. For instance, present-day THz technologies are elaborate enough to perform industrial-scale, nondestructive product quality control,[15–19] and even security screening.[20,21]

In nondestructive testing performed at THz frequencies, there are two conventional approaches: the time-domain spectroscopy[22,23] and the continuous wave (cw) schemes.[24,25] The former is based on irradiating a sample with short electromagnetic pulses and analyzing the resultant transmitted or reflected signal. Although this technique provides detailed information about the sample absorption or reflection spectra over the entire THz frequency band, a typical setup is highly complex and costly, with a rather slow measurement rate. The latter method, on the other hand, is considerably simpler, faster, and more cost-effective, as it allows for implementation of fairly compact and portable, commercially available solutions. Recently, there have been reported a number of cw imagers operating at a single radiation frequency,[25–31] including several systems developed by our group at TeraSense.[32–35]

In this paper, we adapt the aforementioned TeraSense instrumentation to the study of water content in plant leaves. In the proposed arrangement, the incident cw radiation generated with a standard impact avalanche and transit time (IMPATT)-diode source at 100 GHz propagates through a leaf sample and is then detected by an imaging camera,[32,33] which permits the analysis of the transmission pattern of the sample and, hence, of the water distribution inside the leaves. The chosen frequency matches one of the atmospheric microwave windows,[36] ensuring the low loss of the microwave power propagating through the air volume. The suggested measurement approach has several key advantages over conventional destructive techniques, such as thermogravimetric methods. It fully preserves the integrity of the test sample, as THz radiation at moderate power levels has a negligible effect on the plants. Second, it enables remote monitoring of leaves' water content in real-time so that the dynamics of plant hydration could be studied under various conditions. Furthermore, THz imaging technology facilitates the analysis of the spatial distribution of water within the leaves.

2 System Description

In our experiments, we used the system configuration depicted schematically in Fig. 1(a). In this arrangement, the radiation produced by the IMPATT-diode source is emitted from the horn antenna attached directly to the output waveguide flange of the generator. To achieve a nearly nondivergent radiation beam, we used an aspherical polytetrafluoroethylene (PTFE) beam-collimating lens with a focal distance of 50 mm. The beam spot was made sufficiently large to cover the full pixel-array area of the imaging camera. Photographs of both the source and the camera are shown in Figs. 1(b) and 1(c), respectively. The source operated at a fixed output power level of ~80 mW, and a single frequency of 96 GHz with 1 MHz linewidth, as determined by the measurements taken with the Agilent E4407B spectrum analyzer along with the Agilent 11970W harmonic mixer, and the VDI Erickson PM5 power meter.

The heart of the system is its real-time imaging camera [Fig. 1(c)], which relies on a new method of plasmonic detection[37,38] that makes possible ultrafast sensing of THz radiation at room temperature. The camera has an array of 32×32 pixels with 1.5×1.5 mm^2 pitch, and a single-pixel size of 1.3×1.3 mm^2. At 96 to 98 GHz, the effective responsivity of each pixel is 50 ± 10 kV/W, and the corresponding noise equivalent power is 1 nW/Hz$^{1/2}$. The image acquisition rate of the camera was set to 24 frames per second. The overall imaging system is controlled by a personal computer through specially designed software.

To estimate the dynamics and spatial distribution of the water content inside the leaves, we acquired the transmission pattern of several leaf samples with each sample placed directly on the imaging camera. The distance between the leaf surface and the detector array was equal to 4 mm. The power of the incident beam was normalized by a reference image recorded when no object was present on the camera. Figures 1(d) and 1(e) show a photo of a tree leaf and its sub-THz

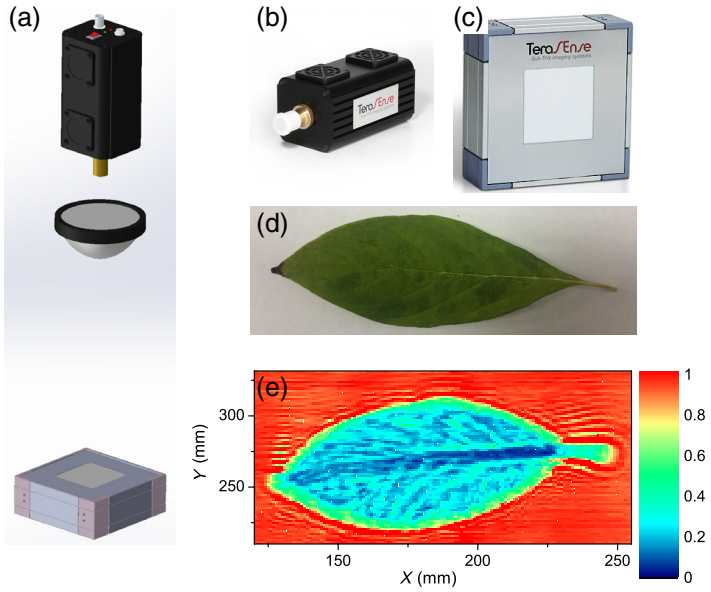

Fig. 1 (a) Schematic illustration of the experimental setup. The radiation beam produced by the IMPATT-diode source is collimated by a PTFE lens with a focal distance of 50 mm. The power distribution within the beam is probed with the imaging camera. (b) and (c) Photos of the camera and the IMPATT source. (d) and (e) A regular, visible light photo, and a sub-THz image of a tree leaf. Image colors indicate the transmission coefficient values.

image reconstructed from several 32×32 pixels images. The colors indicate the transmission coefficient values. Notably, the inner structure of the leaf is clearly resolved in the obtained image. In our investigation, we focused primarily on two plant species that are important in agriculture, namely clover and grass. We measured the transmission patterns of different leaves over several days while the plants growing in the pots were subject to water-restricted conditions.

3 Measurement Results

Figure 2 shows transmission data for three clover leaves tested during a 6-day period without watering. The blue open symbols represent dependence of transmission averaged over the

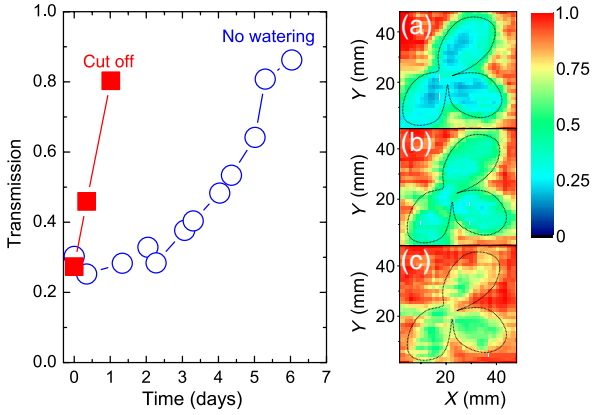

Fig. 2 Changes in the transmission of a sub-THz signal through the leaf of clover. The blue curve with empty circles denotes the time evolution of the transmission through the leaf samples of a plant subject to water restricted conditions. The respective sub-THz images of the clover leaves, (a)–(c) illustrate different hydration levels measured on the first, third, and fifth days of the experiment. Image colors correspond to the value of the transmittance. The red curve with solid points represents an analogous dependence for the leaf cut off from the same plant.

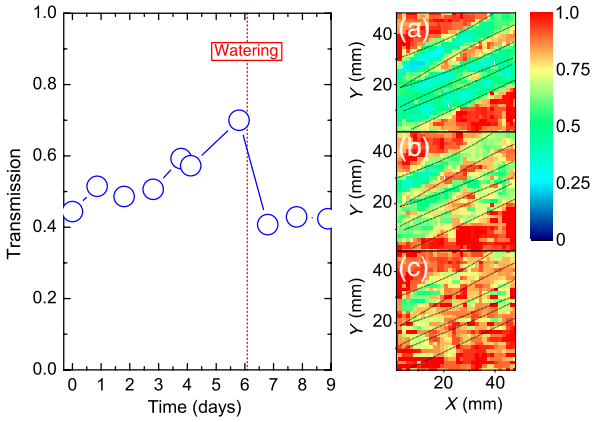

Fig. 3 Changes in the transmission of a sub-THz signal through the grass blades. The blue curve with empty circles corresponds to the mean transmission values. The red-dashed line marks the moment of watering the plant. Sub-THz images (a)–(c) illustrate various degrees of hydration of the grass blades, recorded on the first, fourth, and sixth days of the experiment, prior to the indicated watering of the plant. Image colors designate the value of the transmittance.

number of camera pixels. In order to average the transmission coefficient, three areas of a leaf were taken, in particular, rectangular sections of 5×6 pixels in size, chosen approximately at the center of each leaf. Then, transmission values of all those pixels were averaged giving the solid line in Fig. 2. Over the entire test period, the blue curve illustrates a marked change in the transmission that almost tripled in value after 6 days without watering the plant, which reflects a substantial decrease in the leaf water content. Notably, there is a plateau with approximately constant transmission value during the first 3 days and the subsequent rise. Figures 2(a)–2(c) include sub-THz images denoting the transmission patterns of the clover leaves recorded on the first, third, and fifth days of the experiment. The images help to visualize the progressive reduction in water content inside the leaves, making it evident that the central parts of the leaves dry out at a lower rate than their periphery. Thus, application of sub-THz imaging is essential to perform correct water content evaluation as a leaf position may be changed.

For comparison, a similar experiment was carried out with the leaves separated from the same clover plant. As indicated by the red curve, cutting the leaf off causes a surge in its transmission value, signifying rapid dehydration of the detached leaf within a single day.

Another point of interest in our study was to examine the leaf water dynamics during its dehydration-watering cycle. Figure 3 shows the transmission of three grass-blade samples over a 9-day test period with a single intermediate watering on day 6. In this case, the transmission estimate was obtained following the same averaging procedure as described above. The three images in the figure represent the transmission patterns recorded on the first, fourth, and sixth days of the experiment, during which period no water was supplied to the plant. Similar to the previous results for the clover leaves, we can see a well-established trend of an increasing transmission coefficient related to the gradual dehydration of the grass leaves.

When the grass was watered at the end of day 6, as marked by a red-dashed line, the data indicate a prompt return to the initial transmission level, implying that the water content in the grass leaves is fully restored less than a day after watering.

Since the transmission coefficient is related directly to the measure of water in plant leaves, in many agricultural applications, it is sufficient to know its value, without converting it into the actual water content. Hence, this figure can be used as a basis for estimating the other parameters of interest, including the optimal watering schedule of the crops.

4 Conclusion

In conclusion, the TeraSense imaging system composed of an IMPATT-diode source, a condenser lens, and an imaging camera was adapted to performing the quantitative analysis of the temporal evolution and spatial distribution of water in clover and grass leaves. The water content

of leaf samples was estimated by measuring the transmission of 100 GHz radiation through the leaves. We observed the time changes in the transmission coefficient when the plants were subject to water-restricted conditions. We show that watering the plants after prolonged dehydration results in prompt restoration of the transmission parameter to its initial value. The presented experimental findings demonstrate that TeraSense imaging instrumentation is fully capable of monitoring the hydration state of plants. Further development in this field of research may involve raising the radiation frequency to a higher band of 300 GHz to enhance spatial resolution. In this case, the size of the pixel would be decreased correspondingly to avoid the loss of the spatial resolution. Moreover, imaging in reflection mode may enable real-time, continuous remote monitoring and control of the plants' hydration status.

Acknowledgments

The work was supported by the Russian Science Foundation Grant No. 19-72-30003. Disclosures: The authors have no potential conflicts of interest to disclose.

References

1. T. Crowe et al., "Terahertz sources and detectors and their application to biological sensing," *Philos. Trans. A Math. Phys. Eng. Sci.* **362**, 365–377 (2004).
2. T. Löffler et al., "Terahertz dark-field imaging of biomedical tissue," *Opt. Express* **9**(12), 616–621 (2001).
3. P. Knobloch et al., "Medical THz imaging: an investigation of histo-pathological samples," *Phys. Med. Biol.* **47**(21), 3875–3884 (2002).
4. H. Ge et al., "Identification of wheat quality using THz spectrum," *Opt. Express* **22**, 12533–12544 (2014).
5. W. Xu et al., "Discrimination of transgenic rice containing the cry1ab protein using terahertz spectroscopy and chemometrics," *Sci. Rep.* **5**, 11115 (2015).
6. B. B. Hu and M. C. Nuss, "Imaging with terahertz waves," *Opt. Lett.* **20**(16), 1716–1718 (1995).
7. P. E. Verslues et al., "Methods and concepts in quantifying resistance to drought, salt and freezing, abiotic stresses that affect plant water status," *Plant J.* **45**, 523–539 (2006).
8. J. Xu, K. W. Plaxco, and S. J. Allen, "Absorption spectra of liquid water and aqueous buffers between 0.3 and 3.72 THz," *J. Chem. Phys.* **124**, 036101 (2006).
9. H. J. Liebe, G. A. Hufford, and T. Manabe, "A model for the complex permittivity of water at frequencies below 1 THz," *Int. J. Infrared Millimeter Waves* **12**, 659–675 (1991).
10. D. Mittleman, R. Jacobsen, and M. Nuss, "T-ray imaging," *IEEE J. Sel. Top. Quantum Electron.* **2**, 679–692 (1996).
11. N. Born et al., "Monitoring plant drought stress response using terahertz time-domain spectroscopy," *Plant Physiol.* **164**, 1571–1577 (2014).
12. E. Castro-Camus, M. Palomar, and A. A. Covarrubias, "Leaf water dynamics of arabidopsis thaliana monitored in-vivo using terahertz time-domain spectroscopy," *Sci. Rep.* **3**, 2910 (2013).
13. R. Gente et al., "Determination of leaf water content from terahertz time-domain spectroscopic data," *J. Infrared, Millimeter, Terahertz Waves* **34**, 316–323 (2013).
14. G. G. Hernandez-Cardoso et al., "Terahertz imaging for early screening of diabetic foot syndrome: a proof of concept," *Sci. Rep.* **7**, 42124 (2017).
15. S. Wietzke et al., "Industrial applications of THz systems," *Proc. SPIE* **7385**, 738506 (2009).
16. M. Schwerdtfeger et al., "Beating the wavelength limit: three-dimensional imaging of buried subwavelength fractures in sculpture and construction materials by terahertz time-domain reflection spectroscopy," *Appl. Opt.* **52**, 375–380 (2013).
17. H. Zhong et al., "Nondestructive defect identification with terahertz time-of-flight tomography," *IEEE Sens. J.* **5**, 203–208 (2005).
18. A. I. Hernandez-Serrano et al., "Quality control of leather by terahertz time-domain spectroscopy," *Appl. Opt.* **53**, 7872–7876 (2014).

19. D. Banerjee et al., "Diagnosing water content in paper by terahertz radiation," *Opt. Express* **16**, 9060–9066 (2008).
20. K. Kawase et al., "Non-destructive terahertz imaging of illicit drugs using spectral fingerprints," *Opt. Express* **11**, 2549–2554 (2003).
21. Y. C. Shen et al., "Detection and identification of explosives using terahertz pulsed spectroscopic imaging," *Appl. Phys. Lett.* **86**, 241116 (2005).
22. M. Tonouchi, "Cutting-edge terahertz technology," *Nat. Photonics* **1**, 97–105 (2007).
23. P. Jepsen, D. Cooke, and M. Koch, "Terahertz spectroscopy and imaging: modern techniques and applications," *Laser Photonics Rev.* **5**, 124–166 (2010).
24. S. Hadjiloucas, L. Karatzas, and J. Bowen, "Measurements of leaf water content using terahertz radiation," *IEEE Trans. Microwave Theory Tech.* **47**, 142–149 (1999).
25. N. Karpowicz et al., "Compact continuous-wave subterahertz system for inspection applications," *Appl. Phys. Lett.* **86**, 054105 (2005).
26. A. Dobroiu et al., "Terahertz imaging system based on a backward-wave oscillator," *Appl. Opt.* **43**, 5637–5646 (2004).
27. Q. Song et al., "Fast continuous terahertz wave imaging system for security," *Opt. Commun.* **282**, 2019–2022 (2009).
28. B. Breitenstein et al., "Introducing terahertz technology into plant biology: a novel method to monitor changes in leaf water status," *J. Appl. Bot. Food Qual.* **84**, 158–161 (2011).
29. Y. F. Sun et al., "Room temperature gan/algan self-mixing terahertz detector enhanced by resonant antennas," *Appl. Phys. Lett.* **98**, 252103 (2011).
30. Y. F. Sun et al., "High-responsivity, low-noise, room-temperature, self-mixing terahertz detector realized using floating antennas on a ganbased field-effect transistor," *Appl. Phys. Lett.* **100**, 013506 (2012).
31. H. Qin et al., "Detection of incoherent terahertz light using antenna-coupled high-electron-mobility field-effect transistors," *Appl. Phys. Lett.* **110**, 171109 (2017).
32. G. Tsydynzhapov et al., "Commercial sub-THz video camera," in *20th Int. Disp. Workshops 2013, IDW 2013*, pp. 1413–1414 (2013).
33. V. Muravev et al., "High-speed THz semiconductor imaging camera," in *38th Int. Conf. Infrared, Millimeter, and Terahertz Waves* (2013).
34. V. M. Muravev et al., "New terahertz imaging system for industrial applications," in *41st Int. Conf. Infrared, Millimeter, and Terahertz Waves* (2016).
35. G. E. Tsydynzhapov et al., "New terahertz security body scanner," in *43rd Int. Conf. Infrared, Millimeter, and Terahertz Waves* (2018).
36. M. Klein and A. J. Gasiewski, "The sensitivity of millimeter and sub-millimeter frequencies to atmospheric temperature and water vapor variations," in *Sens. Manag. Environ. IEEE Int. Geosci. and Remote Sens., IGARSS'98, Symp. Proc.*, IEEE, vol. 2, pp. 568–571 (1998).
37. V. M. Muravev and I. V. Kukushkin, "Plasmonic detector/spectrometer of subterahertz radiation based on two-dimensional electron system with embedded defect," *Appl. Phys. Lett.* **100**, 082102 (2012).
38. V. M. Muravev et al., "On the response time of plasmonic terahertz detectors," *J. Exp. Theor. Phys. Lett.* **103**, 792–794 (2016).

Anton V. Shchepetilnikov received his BSc and MSc degrees in applied physics and mathematics from Moscow Institute of Physics and Technology, Moscow, Russia, in 2010 and 2012, respectively. He received his PhD in solid state physics from Institute of Solid State Physics, Chernogolovka, Russia, in 2016. He is currently a senior scientist at Institute of Solid State Physics, Chernogolovka, Russia, and also a senior engineer at Terasense Group Inc., San Jose, USA. His current research interests include spin physics in low-dimensional systems and subterahertz imaging applications.

Alexey M. Zarezin received his BSc degree in applied physics and mathematics from Moscow Institute of Physics and Technology, Moscow, Russia, in 2019. He is currently pursuing his MSc degree at Moscow Institute of Physics and Technology, Moscow, Russia. He is also an engineer at Institute of Solid State Physics, Chernogolovka, Russia, and an engineer at Terasense Group Inc., San Jose, USA. His current research interests include plasmons in low-dimensional systems and sub-terahertz imaging applications.

Viacheslav M. Muravev received his BSc and MSc degrees in applied physics and mathematics from Moscow Institute of Physics and Technology, Moscow, Russia, in 2005 and 2007, respectively. He received his PhD in solid state physics from Institute of Solid State Physics, Chernogolovka, Russia, in 2010. He is currently a senior scientist at Institute of Solid State Physics, Chernogolovka, Russia, and also a vice president of Terasense Group Inc., San Jose, USA. His current research interests include plasmons in low-dimensional systems and sub-terahertz imaging applications.

Pavel A. Gusikhin, received his BSc and MSc degrees in applied physics and mathematics from Moscow Institute of Physics and Technology, Moscow, Russia, in 2009 and 2011, respectively. He received his PhD degree in solid state physics from Institute of Solid State Physics, Chernogolovka, Russia, in 2016. He is currently a scientist at Institute of Solid State Physics, Chernogolovka, Russia, and also a senior engineer at Terasense Group Inc., San Jose, USA. His current research interests include plasmons in low-dimensional systems and sub-terahertz imaging applications.

Igor V. Kukushkin is a chief scientific researcher at the Institute of Solid State Physics, Chernogolovka, Russia, and also a president of Terasense Group Inc., San Jose, USA. He received his PhD in solid state physics from Institute of Solid State Physics, Chernogolovka, Russia, in 1983. In 2016 he was elected a member of the Russian Academy of Sciences (General Physics and Astronomy Division). His current research interests include low-temperature physics of low-dimensional systems and sub-terahertz imaging applications.